Bull. Chem. Soc. Jpn. Vol. 83, No. 12, 1439–1446 (2010)

BCSJ Award Article

Redox Behavior and Electrochemical Catalytic Function of B_{12}–Hyperbranched Polymer

Keishiro Tahara,[1] Hisashi Shimakoshi,[1] Akihiro Tanaka,[1,2] and Yoshio Hisaeda*[1,3]

[1]Department of Chemistry and Biochemistry, Graduate School of Engineering, Kyushu University, Fukuoka 819-0395

[2]Synthesis Research Department, Chemical Research Laboratory, Nissan Chemical Industries, Ltd., Funahashi 274-8507

[3]International Research Center for Molecular Systems (IRCMS), Kyushu University, Fukuoka 819-0395

Received August 11, 2010; E-mail: yhisatcm@mail.cstm.kyushu-u.ac.jp

The electrochemical behavior of a covalently functionalized hyperbranched polymer with a vitamin B_{12} derivative (B_{12}–HBP) was investigated by cyclic voltammetry and UV–vis spectroscopy combined with bulk electrolysis in *N*,*N*-dimethylformamide. The B_{12}–HBP showed excellent properties for a homogeneous catalyst such as the good accessibilities of the cobalt centers in B_{12}–HBP to an electrode and substrates and the maintained supernucleophilicity of the Co(I) species to alkyl halides. The cobalt-methylated B_{12}–HBP was newly synthesized, and its electrochemical behavior was also investigated by cyclic voltammetry. Furthermore, B_{12}–HBP was used as an electrochemical degradation catalyst for 1,1,1-trichloro-2,2-bis(4-chlorophenyl)ethane (DDT). This work presents the first electrocatalysis study of a catalytically active transition-metal complex on a homogeneous dendritic support and investigates the suitability of the present B_{12}–HBP system for electrochemical dehalogenation.

There has been increasing attention to the use of soluble polymers for homogeneous catalyst supports as a potential alternative to traditional solid-phase syntheses in recent years.[1–4] In particular, soluble branched polymers, such as dendrimers and hyperbranched polymers (HBPs), have been widely investigated as homogeneous supports for catalytically active transition-metal complexes, which are either covalently attached to the core/periphery moiety or noncovalently incorporated.[5,6] These microscopically heterogeneous and dendritic polymers offer several advantages such as their ready removal from the products,[7] good accessibilities to catalytic centers,[8] and dendritic effects on the catalyst activity/selectivity.[9,10] In other words, they can combine the advantages of homogeneous and heterogeneous catalysis as promising scaffolds which effectively organize catalytic sites on their nanosized structure but do not hinder the catalytic process. However, the application of these branched polymers to electrochemical molecular transformations represents an almost unexplored area, although the electrochemical activation of the transition-metal catalysts is a beneficial method to develop good redox catalysis systems.[11]

Vitamin B_{12} and derivatives can acquire three formal oxidation states of cobalt, and each oxidation state has quite difference ligand accepting abilities (i.e., octahedral, square pyramidal, or square planar for Co(III), Co(II), or Co(I), respectively).[12,13] Such a redox- and coordination-rich chemistry plays a critical role in the cobalamin-dependent enzymatic reactions in vivo[14,15] and in a number of chemical transformations in vitro.[16–22] We have been dealing with a hydrophobic vitamin B_{12}, heptamethyl cobyrinate perchlorate, $[Cob(II)7C_1ester]ClO_4$ (**1**)[23] as shown in Scheme 1 and succeeded in various electroorganic transformations.[24–28] These reactions are based on the easy accessibility of **1** to the Co(I) species ($E^0(Co^{II}/Co^{I}) = -0.64$ V vs. SCE),[24] the supernucleophilicity of the resulting low-valent species to alkyl halides and the electrochemical cobalt–carbon bond cleavage of the Co(III)-alkylated complex. In the previous work, our interest in the immobilization of redox- and coordination-rich metal

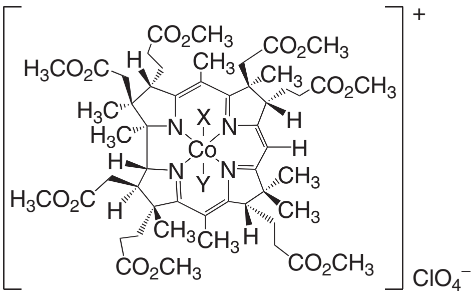

Hydrophobic vitamin B_{12}

X = Y = none $[Cob(II)7C_1ester]ClO_4$ (**1**)

X = CH_3, Y = H_2O $[(H_2O)(CH_3)Cob(III)7C_1ester]ClO_4$ (**2**)

Scheme 1.

Published on the web November 20, 2010; doi:10.1246/bcsj.20100221

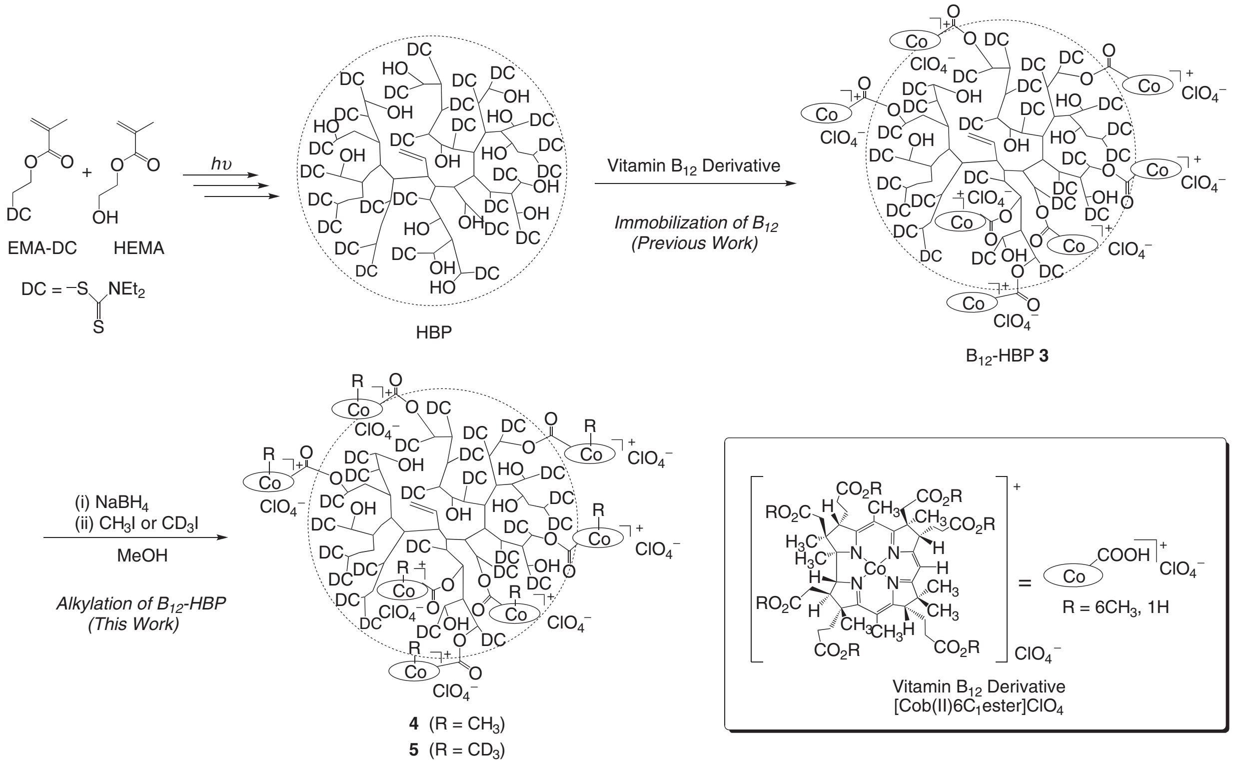

Scheme 2. Syntheses of CH_3– and CD_3–B_{12}–HBP **4** and **5**.

complexes on a soluble dendritic support has motivated us to prepare a covalently functionalized hyperbranched polymer with a vitamin B_{12} derivative (B_{12}–HBP) as shown in Scheme 2.[29,30] Using a recent advanced technique for polymer syntheses followed by a modification procedure, the catalytic sites of B_{12} were effectively introduced along the highly branched polymeric backbone to afford the multimetallic catalytic nanomaterial with a high density of cobalt centers.

In this study, we report the redox behavior of B_{12}–HBP and its application to the electrolysis of an alkyl halide. We also report a method for alkylation of the cobalt center in B_{12}–HBP and the electrochemical behavior of the resulting alkylated B_{12}–HBP. This work presents the first electrocatalysis study of a catalytically active transition-metal complex on a homogeneous dendritic support and investigates the suitability of the present B_{12}–HBP system for electrochemical dehalogenation.

Experimental

Materials. All solvents and chemicals used in the syntheses were of reagent grade and were used without further purification. For electrochemical studies, *N*,*N*-dimethylformamide (DMF) was stirred for one day in the presence of BaO under a nitrogen atmosphere and distilled under reduced pressure. Tetra-*n*-butylammonium perchlorate (n-Bu_4NClO_4) was purchased from Nakalai Chemicals (special grade) and dried at room temperature under vacuum before use. 1,1,1-Trichloro-2,2-bis(4-chlorophenyl)ethane, DDT, was purchased from Tokyo Kasei Kogyo (TCI). The silica gel used for column chromatography was Silica Gel 60N (spherical: 60–210 µm, neutral) purchased from Kanto Chemical Co., Inc. [Cob(II)7-C_1ester]ClO_4 (**1**) was synthesized according to the previously reported method.[23] B_{12}–HBP **3** used in this study was synthesized and characterized in the previous paper as follows (Scheme 2).[30] **3**: HBP having OH groups with a 1:1 composite of 2-(*N*,*N*-diethyldithiocarbamoyl)ethyl methacrylate (EMA-DC) and 2-hydroxyethyl methacrylate (HEMA) ($M_w = 98400$, $M_w/M_n = 7.69$ determined by GPC-MALS (multi-angle light scattering)) was covalently functionalized by esterification with a vitamin B_{12} derivative having a carboxylic acid, [Cob(II)-6C_1ester]ClO_4, to afford B_{12}–HBP **3**. The content of B_{12} in **3** was 0.47 mmol g^{-1} based on the cobalt content of B_{12} determined by atomic absorption spectrometry. Based on the elemental anaysis, the chemical formula was determined as follows. Calcd for $[C_{11}H_{19}NO_2S_2]_{251}[C_6H_{10}O_3]_{156}[C_{57}H_{79}ClCoN_4O_{20}]_{95}$: C, 53.86; H, 6.86; N, 4.35%. Found: C, 53.73; H, 7.12; N, 4.33%. 39% of the OH groups of the HBP were esterified with the vitamin B_{12} derivative.

General Analyses and Measurements. The UV–vis absorption spectra were measured on a Hitachi U-3300 spectrometer at room temperature. The ^{1}H NMR spectra were recorded on a Bruker Avance 500 spectrometer installed at the Center of Advanced Instrumental Analysis in Kyushu University, and the chemical shifts (in ppm) were referenced relative to the residual protic solvent peak. Gel permeation chromatography (GPC) was carried out on a Hitachi High-Tech Fielding Co., Ltd., HPLC EZChrom Elite combined with an L-2455 DAD attachment, using three connected columns, Shodex KD-805, -804, and -802, with DMF containing LiBr as an eluent. The samples were treated with KCN for the dicyanation of the cobalt center of B_{12} before analyses. Photochemical reactions were performed by an apparatus with a 200 W tungsten lamp for visible light irradiation.

Synthesis of CH_3–B_{12}–HBP 4. Compound **3** (25 mg; B_{12} derivative, 1.2×10^{-5} mol) was dissolved in 10 mL of acetonitrile, and 40 mL of distilled water and 50 mL of methanol were added to this solution (Scheme 2). The solution was deoxygenated by bubbling nitrogen gas through it for 15 min at room temperature, and sodium tetrahydroborate (50 mg, 1.3 mmol) dissolved in 3 mL of methanol was added to the deoxygenated solution with vigorous stirring under nitrogen atmosphere. The following operations were carried out in the dark. When the solution turned dark green, iodomethane (CH_3I) (220 mg, 1.55 mmol) was added to it. The resulting solution was stirred for 5 min at room temperature, and 2 mL of 60% aqueous perchloric acid was added carefully to decompose excess sodium tetrahydroborate. The resulting product was extracted with dichloromethane and washed with distilled water. After drying over anhydrous Na_2SO_4, the organic layer was evaporated to dryness. The residue was reprecipitated from $CHCl_3$ upon addition of *n*-hexane to afford a brown powder. Yield: 24 mg. UV–vis (in CH_2Cl_2): [λ_{max}/nm], 263, 283, 375, 458; ^{1}H NMR ($CDCl_3$, 500 MHz): δ −0.25 (Co–CH_3), 1.3 (–N($CH_2CH_3)_2$), 3.5–3.9 (broad, –NCH_2CH_3, –CH_2CH_2SC(S)N–, –CH_2CH_2OH, C(O)OCH_3 of B_{12}), 4.00 (–CH_2CH_2SC(S)N–), 4.1–4.6 (broad, –CH_2CH_2OH, –NCH_2CH_3, –C(O)OCH_2CH_2-OC(O)–), 5.4 (C(10)–*H* of corrin).

Synthesis of CD_3–B_{12}–HBP 5. Compound **3** (20 mg) was used and the deuterated compound **5** was synthesized in the same manner as for **4**, except for the use of iodomethane-d_3 (CD_3I). Yield: 19 mg. UV–vis (in CH_2Cl_2): [λ_{max}/nm], 263, 302, 377, 458; ^{1}H NMR ($CDCl_3$, 500 MHz): δ 1.3 (–N($CH_2CH_3)_2$), 3.5–3.9 (broad, –NCH_2CH_3, –CH_2CH_2SC(S)N–, –CH_2CH_2OH, C(O)OCH_3 of B_{12}), 4.00 (–CH_2CH_2SC(S)N–), 4.1–4.6 (broad, –CH_2CH_2OH, –NCH_2CH_3, –C(O)OCH_2CH_2-OC(O)–), 5.4 (C(10)–*H* of corrin).

Electrochemical Measurements. All voltammetric experiments were carried out with a BAS CV50W electrochemical analyzer. Experiments were performed using a conventional three-electrode system. A platinum wire (1.6 mm in diameter) was employed as a counter electrode, a glassy carbon electrode (3.0 mm in diameter) as a working electrode, and an Ag/AgCl (3.0 M NaCl) electrode as a reference electrode. Nonaqueous DMF solutions containing **3** and *n*-Bu_4NClO_4 (0.1 M) were deaerated prior to each measurement, and a nitrogen atmosphere was maintained inside the cell throughout each measurement. All measurements were carried out at room temperature. The $E_{1/2}$ value of ferrocene/ferrocenium (Fc/Fc^+) was 0.56 V vs. Ag/AgCl with this setup.

The controlled-potential electrolysis of **3** was carried out at −1.20 V vs. Ag/AgCl and followed by UV–vis spectroscopy under nitrogen atmosphere using an optical thin-layer quartz cell. The working and counter electrodes made from platinum mesh were used along with an Ag/AgCl reference electrode. The applied potential between the working and reference electrodes during the electrolysis was maintained constant with a Hokuto Denko HA-501 potentiostat/galvanostat.

The controlled-potential electrolysis of DDT was carried out at −1.50 V vs. Ag/AgCl in the presence of B_{12}–HBP **3** or the monomeric B_{12} derivative **1** in a cylindrical three-electrode cell which was divided into two internal compartments with a single sheet of a microporous polypropylene membrane equipped with a platinum mesh cathode and a zinc plate anode (1×3 cm^2) under a nitrogen atmosphere. The applied potential between the working and reference electrodes during the electrolysis was maintained constant with a Hokuto Denko HA-501 potentiostat/galvanostat, and the reaction was monitored on a Hokuto Denko HF-201 coulomb/ampere-hour meter. Initial concentrations: $[B_{12}] = 2.0 \times 10^{-4}$ M, $[DDT] = 2.5 \times 10^{-2}$ M; DMF solution containing 0.1 M *n*-Bu_4NClO_4. After the electrolysis, DMF was removed by evaporation under reduced pressure and 30 mL of $CHCl_3$ was added to the residue. The chloroform layer was washed with water (3×40 mL) to remove DMF completely and dried with Na_2SO_4. The filtrate was then concentrated to dryness. The residue was passed through a silica gel short column eluting with $CHCl_3$ to remove *n*-Bu_4NClO_4 and **3** or **1**, and the products were then analyzed by NMR.

Results and Discussion

Redox Behavior of B_{12}–Hyperbranched Polymer. To obtain new insight into the effect of a homogeneous dendritic support on the redox processes of the immobilized transition-metal complex, we first investigated the redox behavior of B_{12}–HBP **3** by means of cyclic voltammetry. A reversible redox wave was observed at −0.48 V vs. Ag/AgCl in DMF as shown in Figure 1a. In order to identify the complex species formed during the redox process, the controlled-potential electrolysis of **3** was carried out at −1.20 V vs. Ag/AgCl. This electrochemical reduction was monitored by UV–vis absorption spectroscopy, which showed characteristic strong absorption at 390 nm indicative of the Co(I) species of the vitamin B_{12} derivative as shown in Figure 2. Thus, the observed redox wave is ascribed to the Co(II)/Co(I) redox couple of B_{12} moieties in **3**. The obtained half-wave potential $E_{1/2}$ (Co(II)/Co(I)) of **3** was almost equal to that of the monomeric vitamin B_{12} derivative **1** as shown in Table 1.[24] This result indicates that the B_{12} moieties of **3** are efficiently solvated and that the microenvironment of the hyperbranched polymer does not affect the intrinsic redox property of the constituent B_{12} derivative. Such an indication of the local environment in **3** is consistent with the fact that the weight of the B_{12} moieties of B_{12}–HBP **3** accounts for ca. 50% of the entire weight of **3**, as well as the fact that the solubility of **3** in organic solvents is different from that of the unmodified HBP, but similar to that of the monomeric B_{12} **1**.[29,30] The peak currents of **3** increased in proportion to the square root of the scan rate over a range of scan rates from 20 to 500 mV s^{-1} as shown in Figure 1b. This good reversibility clearly indicates that a fast electron transfer proceeds by the diffusion of B_{12}–HBP to the electrode. The obtained diffusion coefficient of B_{12}–HBP **3** was smaller than that of the monomeric vitamin B_{12} derivative **1**, reflecting the molecular-weight difference in both compounds. In spite of the requirement for such a diffusion process of the macromolecule **3**, as well as some steric hindrance of the polymer support to the cobalt centers, an almost quantitative reduction of the cobalt centers of B_{12}–HBP **3** was achieved on the bulk electrolysis time scale described above. This result implies that the cobalt centers can get into a position accessible to the electrode with a local morphology change in **3** because the B_{12} units are covalently immobilized on the relatively flexible poly(ethyl

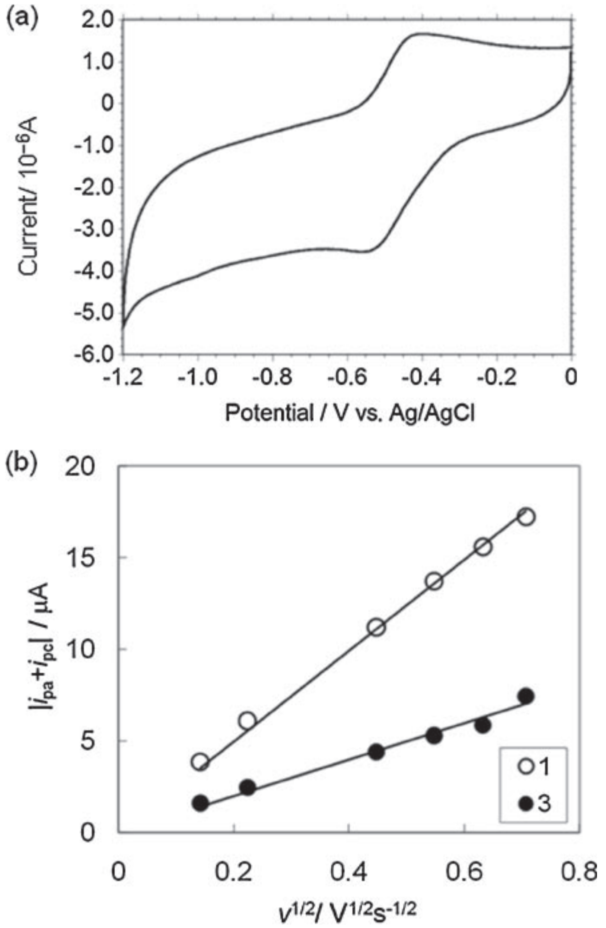

Figure 1. (a) Cyclic voltammograms of B_{12}–HBP **3** ($[B_{12}] = 5.0 \times 10^{-4}$ M) in DMF containing 0.10 M n-Bu_4NClO_4, sweep rate: 100 mV s^{-1}. (B) The scan rate dependence on the peak current for the Co(II)/Co(I) couple of B_{12}–HBP **3** and the monomeric B_{12} **1**.

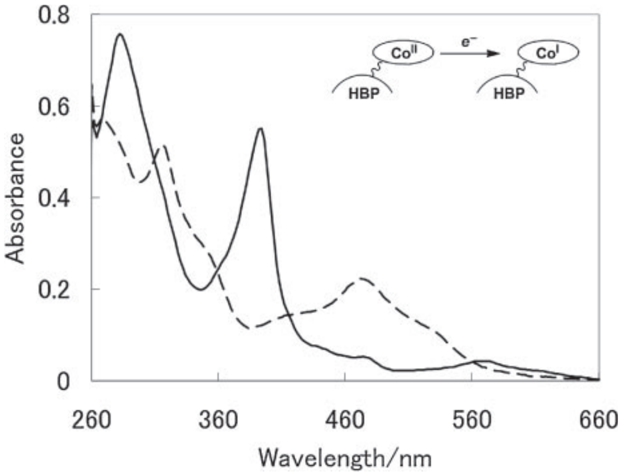

Figure 2. UV–vis absorption spectra of a DMF solution containing B_{12}–HBP **3** ($[B_{12}] = 5.0 \times 10^{-4}$ M) and n-Bu_4NClO_4 (0.10 M) before (broken line) and after (solid line) the controlled potential electrolysis at −1.20 V vs. Ag/AgCl.

Table 1. Redox Potentials and Diffusion Constants for B_{12}–HBP **3** and Monomeric B_{12} **1**

Compounds	$E_{1/2}$ (Co(II)/Co(I)) /V vs. Ag/AgCl	$E_{1/2}$ (Co(II)/Co(I)) /V vs. Fc/Fc^+	Diffusion constants /10^6 cm^2 s^{-1} [a)]
B_{12}–HBP **3**	−0.48	−1.04	0.27[b)]
Monomeric B_{12} **1**	−0.49	−1.05	1.7

a) Calculated based on the scan rate dependence on the peak current for the Co(II)/Co(I) couple of B_{12}. b) Determined based on the concentration of B_{12} units in **3** rather than those of B_{12}–HBP nanoparticle.

methacrylate)s backbone. In the pioneering work on multimetallic catalytic systems, it has been proposed that, in nickelated carbosilane dendrimers, electron transfers occur inside the dendrimer support between the constituent nickel centers (closest distances about 0.8–1.1 nm), resulting in the formation of mixed-valance nickel sites.[9] Similar electron transfers between the constituent B_{12} moieties inside the B_{12}–HBP nanoparticle might be possible due to the high density of the metal centers (ca. 100 cobalt sites in a particle in the range of 3 to 5 nm)[30] and might contribute to the quantitative reduction of cobalt centers of **3** by compensating for some steric hindrance of more interior B_{12} moieties to the electrode. These electrochemical studies show the suitability of the present hyperbranched copolymer for the use as a homogeneous scaffold in combination with a good redox mediator.

The reactivity of the Co(I) species of B_{12}–HBP with an organic halide was also investigated by cyclic voltammetry. In the presence of an excess of iodomethane (CH_3I), a new irreversible and strong reduction wave was observed at ca. −1.4 V vs. Ag/AgCl as shown in Figure 3a. This voltammetric change indicates that the electrochemically activated B_{12}–HBP reacted with CH_3I to afford the catalytic current. Similar reduction waves had been obtained for DMF solutions of **1** in the presence of various alkyl halides, which were ascribed to the one-electron reduction of the alkyl–Co(III) complexes, resulting from the oxidative addition of the Co(I) species to the corresponding alkyl halides.[25] This electrolysis of the alkyl–Co(III) complexes had been shown to induce the reductive cobalt–carbon bond cleavage, resulting in regeneration of the Co(I) species and the subsequent oxidative addition to alkyl halides.[25] Combined with the previous reports of the monomeric B_{12}, the present voltammetric study suggests that the cobalt centers of **3** are accessible to an alkyl halide and that the B_{12}–HBP maintains the supernucleophilicity of the Co(I) species. The resulting organometallic Co(III)–C bond of the B_{12}–HBP is reductively cleaved under electrochemical condition. In order to further investigate the reactivity of this organocobalt species of B_{12}–HBP, the cobalt-methylated polymer **4** (CH_3–B_{12}–HBP) was synthesized and characterized from photochemical and electrochemical points of view as described below.

Synthesis and Characterization of CH_3–B_{12}–Hyperbranched Polymer. Methylation of the cobalt centers of **3** was performed using a procedure similar to that reported for the monomeric B_{12} derivative **1**[31] as shown in Scheme 2. A reduction in cobalt centers of **3** with sodium tetrahydroborate in aqueous methanol afforded a green solution, which showed a

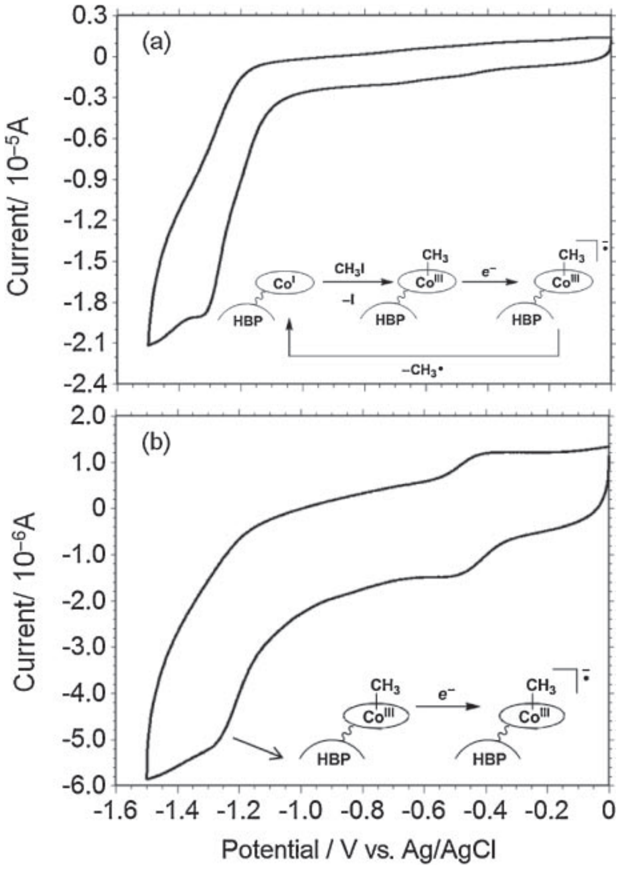

Figure 3. Cyclic voltammograms of (a) B_{12}–HBP **3** ($[B_{12}] = 5.0 \times 10^{-4}$ M) in the presence of 5.0×10^{-3} M CH_3I and (b) CH_3–B_{12}–HBP **4** ($[B_{12}] = 5.0 \times 10^{-4}$ M) in DMF containing 0.10 M n-Bu_4NClO_4, sweep rate: 100 mV s^{-1}.

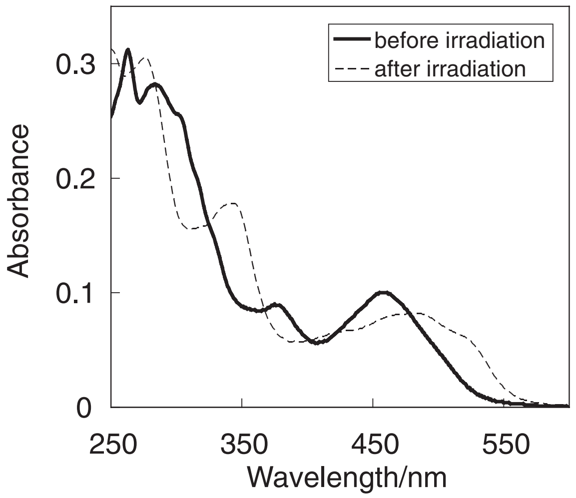

Figure 4. UV–vis absorption spectra of **4** in CH_2Cl_2 before and after irradiation with visible light, $[B_{12}] = 9.7 \times 10^{-6}$ M.

characteristic strong absorption at 390 nm indicative of the supernucleophile Co(I) species as shown in Figure S1. A subsequent reaction with iodomethane immediately afforded a brown solution. The target compound **4** was extracted to dichloromethane and reprecipitated upon addition of hexane to give a brown powder. The UV–vis absorption spectrum of **4** showed the typical shape for the monomeric methyl B_{12} derivative **2**[31] as shown in Figure 4. This spectrum clearly indicates that the cobalt centers of **3** are accessible to the organic halide and that the Co(I) species of B_{12}–HBP reacted with iodomethane to afford almost quantitative methylation of the cobalt centers of **3** with dehalogenation. The CH_3–B_{12}–HBP **4** showed photosensitivity under an aerobic condition as shown in Figure 4. This spectral change can be ascribed to cleavage of the cobalt–carbon bond of **4**, consistent with a previous report on the monomeric B_{12} **2**.[31]

This photosensitive macromolecule **4** was also investigated by ^{1}H NMR spectroscopy. A peak was observed at −0.25 ppm in the ^{1}H NMR spectrum of **4**, which disappeared after visible light irradiation as shown in Figure 5. Such a peak was not observed in the ^{1}H NMR spectrum of CD_3–B_{12}–HBP **5** resulting from the reaction with iodomethane-d_3 (CD_3I), which showed the photosensitivity as shown Figures S2 and S3. These spectral data clearly indicate that the proton peak of the methyl group coordinating the cobalt centers disappeared due to cleavage of the cobalt–carbon bond in **4**.

The GPC diagram for the photolysis product of **4** revealed that the immobilized B_{12} was not leached from the polymer support and that the retention time of B_{12}–HBP in the diagram was maintained during both the procedures of methylation of **3** and photolysis of **4** as shown in Figure S4. Accordingly, B_{12}–HBP **3** is a promising redox mediator with respect to the enduring immobilization of B_{12} on a stable support.

Redox Behavior of CH_3–B_{12}–Hyperbranched Polymer. The redox behavior of CH_3–B_{12}–HBP **4** was investigated by cyclic voltammetry. An irreversible reduction peak was observed at ca. −1.4 V vs. Ag/AgCl in the cyclic voltammogram of the DMF solution of **4** as shown in Figure 3b. This reduction wave is ascribed to the one-electron reduction of the CH_3–Co(III) complex moieties of **4**, consistent with a previous report on the monomeric methylated B_{12} **2**.[32] This reduction potential is comparable to that of the irreversible reduction wave of **3** in the presence of an excess of CH_3I as shown in Figure 3a. Such a similar voltammetric pattern supports the above-mentioned assignments of the reduction waves of the CH_3–Co(III) complex species of B_{12}–HBP. The electrochemical reactivity of alkyl–Co(III) complexes of B_{12}–HBP, as well as the supernucleophilicity of the Co(I) species of B_{12}–HBP to alkyl halides, would be beneficial for the construction of electrocatalytic dehalogenation cycles. In this context, the electrolysis of an alkyl halide mediated by B_{12}–HBP was performed as described below.

Electrolysis of DDT Mediated by B_{12}–HBP. The redox behavior of B_{12}–HBP **3** in the presence of DDT, which is one of the most problematic POPs (persistent organic pollutants),[33,34] was investigated by cyclic voltammetry aiming at an application of the present B_{12}–HBP nanomaterial as an electrochemical remediation catalyst. An irreversible cathodic peak was observed at ca. −0.6 V vs. Ag/AgCl with a huge amount of catalytic current as shown in Figure 6. The reduction wave at −1.3 V vs. Ag/AgCl is ascribed to the one-electron reduction of the corresponding alkylated complex of B_{12}–HBP resulting

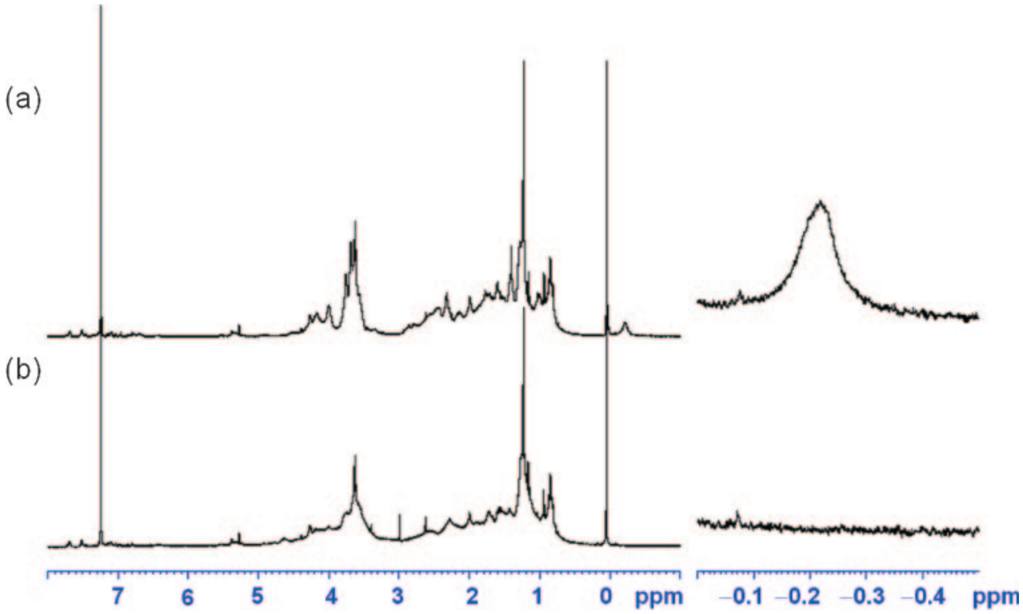

Figure 5. ^{1}H NMR spectra of **4** in $CDCl_3$ (a) before and (b) after irradiation with visible light, $[B_{12}] = 1.3 \times 10^{-3}$ M.

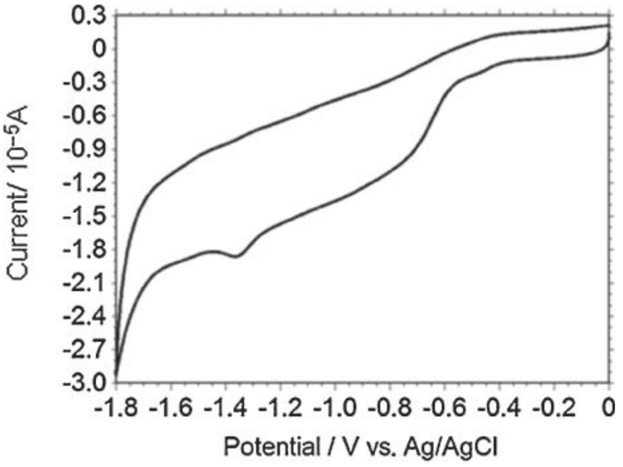

Figure 6. Cyclic voltammograms of B_{12}–HBP **3** ($[B_{12}] = 1.0 \times 10^{-3}$ M) in the presence of DDT (1.0×10^{-3} M) in DMF containing 0.10 M n-Bu_4NClO_4, sweep rate: 200 mV s^{-1}.

Table 2. Electrolysis of DDT Mediated by B_{12}–HBP **3** and the Monomeric B_{12} **1**[a)]

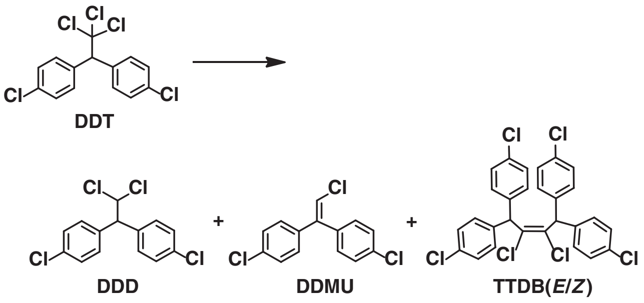

Entry	Catalyst	Charge /F mol^{-1} b)	Conversions /% c)	Product yields/% d)		
				DDD	DDMU	TTDB (*E*/*Z*)
1	B_{12}–HBP **3**	2.0	93	18	31	15/10
2	Monomeric B_{12} **1**	2.0	94	3	53	3/3

a) Controlled-potential electrolyses were carried out in DMF at −1.50 V vs. Ag/AgCl under N_2 atmosphere. Initial concentration: $[B_{12}] = 2.0 \times 10^{-4}$ M, $[DDT] = 2.5 \times 10^{-2}$ M, $[n\text{-}Bu_4NClO_4] = 0.1$ M. b) Electrical charge passed per mol of DDT. c) Conversion was estimated by the recovery of DDT. d) Products were analyzed by NMR.

from the reaction between the Co(I) species and DDT, consistent with a previous report on the monomeric B_{12} **1**.[27]

Based on the initial investigation by cyclic voltammetry, the controlled-potential electrolysis of DDT in the presence of a catalytic amount of B_{12}–HBP **3** was carried out at −1.50 V vs. Ag/AgCl in the DMF solution using a cylindrical three-electrode cell composed of a platinum mesh cathode, a zinc plate anode, and an Ag/AgCl reference electrode. When 2.0 F per mol of DDT had been consumed, the products were extracted from the reaction solution and passed through a silica gel short column to remove **3** and the electrolyte, then analyzed using a similar report procedure[27] as summarized in Table 2. The B_{12}–HBP **3** showed high reactivity with the trihalomethane insecticide, and an effective dehalogenation proceeded as shown in Entry 1 in Table 2. The total turnover number based on the B_{12} content in **3** is 116, and the electrochemical activity of **3** is comparable to that of the monomeric B_{12} **1**. This result implies that almost all the B_{12} moieties participate in the dehalogenation reaction as independent catalytic sites. The catalytic processes at the cobalt centers of **3** were not hindered by the polymeric support, consistent with the above-mentioned good accessibilities of the cobalt centers of B_{12}–HBP to the electrode and an alkyl halide. The present electrolysis study successfully demonstrates the suitability of the present hyperbranched copolymer for use as a homogeneous scaffold in good combination with a catalytically active transition-metal com-

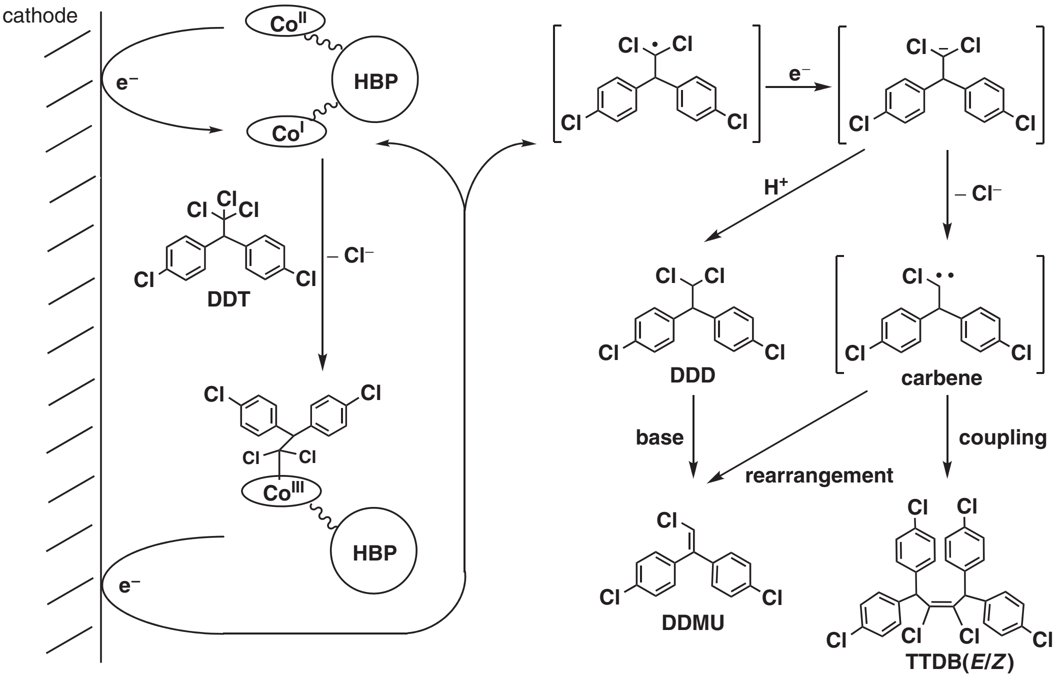

Figure 7. Proposed mechanism for electrolysis of DDT mediated by B_{12}–HBP **3**.

plex, without a decrease in catalytic activity on a substrate. Thus, the B_{12}–HBP system could be applied to remediation technologies to reductively degrade halogenated toxic compounds with nanofiltration membrane reactors reported elsewhere[35] for the facile separation of the catalyst from the product mixture.[36]

The dechlorinated products, DDD (1,1-dichloro-2,2-bis(4-chlorophenyl)ethane), DDMU (1-chloro-2,2-bis(4-chlorophenyl)ethylene), and TTDB (2,3-dichloro-1,1,4,4-tetrakis(4-chlorophenyl)-2-butene), were obtained in the B_{12}–HBP and monomeric B_{12} system, respectively. It is demonstrated that these dehalogenated products are formed via the Cl-eliminated radical species resulting from the reaction of the Co(I) species in our previous report of the DDT dehalogenation mediated by **1** under a similar condition.[27] Based on the present and previous results, the reactions are expected to proceed as shown in Figure 7. The cobalt complex is electrochemically reduced to the Co(I) species, and the corresponding alkylated complex is generated by the reaction between the supernucleophilic Co(I) species and DDT. The alkylated complex is subsequently reduced by electrolysis at this potential to form the Cl-eliminated radical and Co(I) species. A further one-electron reduction of the Cl-eliminated radical species affords a carboanion, which is protonated to give DDD or transferred by a further Cl^- elimination to a carbene resulting in dimerization to form TTDB. DDMU is formed by a rearrangement of the carbene or by the elimination of HCl from DDD. In the present B_{12}–HBP system, it is reasonable to expect that these products (DDD, DDMU, and TTDB) would also be formed via the same radical species because the cobalt centers in **3** function as independent catalytic sites in the DDT dehalogenation reaction. The different product contributions between the B_{12}–HBP and monomeric B_{12} system might reflect the microenvironment of the HBP support. In particular, a somewhat larger yield of TTDB in the B_{12}–HBP system might result from the local environment of **3** with the high density of the cobalt centers which would enhance the dimerization of the carbene intermediate. This is consistent with an increased yield of the coupling product from an alkyl halide (phenethyl bromide) in the previously reported B_{12}–HBP system with a titanium dioxide (TiO_2) photosensitizer under a photochemical condition.[30]

Conclusion

In the present paper, we reported the electrochemical behavior of a covalently functionalized hyperbranched polymer with a vitamin B_{12} derivative (B_{12}–HBP) and successfully demonstrated its application to the electrolysis of an alkyl halide. This work presented the first electrocatalysis study of a catalytically active transition-metal complex on a homogeneous dendritic support and showed the suitability of such a combination for effective catalytic reactions due to good accessibilities to substrates and the electrode surface. This advance would facilitate further application of hyperbranched polymers as homogeneous electrocatalysis supports with promising transition metal complex catalysts for practical uses.

This work was supported by a Grant-in-Aid for Scientific Research on Priority Areas (452 and 460), the Global COE Program "Science for Future Molecular System" from the Ministry of Education, Culture, Sports, Science and Technology (MEXT) of Japan, and a Grant-in-Aid for Scientific Research (No. 21.02310) and a Grant-in-Aid for Scientific Research (A) (No. 21245016) from the Japan Society for the Promotion of Science (JSPS).

Supporting Information

UV–vis and ^{1}H NMR spectroscopic data and GPC profiles of B_{12}–HBP. This material is available free of charge on the web at http://www.csj.jp/journals/bcsj/.

References

1 P. H. Toy, K. D. Janda, *Acc. Chem. Res.* **2000**, *33*, 546.

2 D. E. Bergbreiter, *Chem. Rev.* **2002**, *102*, 3345.

3 T. J. Dickerson, N. N. Reed, K. D. Janda, *Chem. Rev.* **2002**, *102*, 3325.

4 D. E. Bergbreiter, J. Tian, C. Hongfa, *Chem. Rev.* **2009**, *109*, 530.

5 D. Astruc, F. Chardac, *Chem. Rev.* **2001**, *101*, 2991.

6 J. Lu, P. H. Toy, *Chem. Rev.* **2009**, *109*, 815.

7 C. Hajji, R. Haag, *Top. Organomet. Chem.* **2006**, *20*, 149.

8 C. Schlenk, A. W. Kleij, H. Frey, G. van Koten, *Angew. Chem., Int. Ed.* **2000**, *39*, 3445.

9 A. W. Kleij, R. A. Gossage, J. T. B. H. Jastrzebski, J. Boersma, G. van Koten, *Angew. Chem., Int. Ed.* **2000**, *39*, 176.

10 R. Breinbauer, E. N. Jacobsen, *Angew. Chem., Int. Ed.* **2000**, *39*, 3604.

11 J.-M. Savéant, *Chem. Rev.* **2008**, *108*, 2348.

12 B. Kräutler, in *Vitamin B_{12} and B_{12}-Proteins*, ed. by B. Kräutler, D. Arigoni, B. T. Golding, Wiley-VCH, Weinheim, **1998**.

13 G. Wohlfarth, G. Diekert, in *Chemistry and Biochemistry of B_{12}*, ed. by R. Banerjee, Wiley-Interscience, New York, **1999**.

14 T. Toraya, *Chem. Rev.* **2003**, *103*, 2095.

15 K. L. Brown, *Chem. Rev.* **2005**, *105*, 2075.

16 R. Scheffold, G. Rytz, L. Walder, *Mod. Synth. Methods* **1983**, *3*, 355.

17 B. P. Branchaud, G. F. Friestad, *Encyclopedia of Reagents for Organic Synthesis*, **1995**, pp. 5511–5514.

18 D. R. Burris, C. A. Delcomyn, M. H. Smith, A. L. Roberts, *Environ. Sci. Technol.* **1996**, *30*, 3047.

19 C. K. Njue, B. Nuthakki, A. Vaze, J. M. Bobbitt, J. F. Rusling, *Electrochem. Commun.* **2001**, *3*, 733.

20 J. Shey, C. M. McGinley, K. M. McCauley, A. S. Dearth, B. T. Young, W. A. van der Donk, *J. Org. Chem.* **2002**, *67*, 837.

21 F. Sun, T. Darbre, *Org. Biomol. Chem.* **2003**, *1*, 3154.

22 Y. Hisaeda, *Bull. Jpn. Soc. Coord. Chem.* **2009**, *54*, 10.

23 Y. Murakami, Y. Hisaeda, A. Kajihara, *Bull. Chem. Soc. Jpn.* **1983**, *56*, 3642.

24 Y. Murakami, Y. Hisaeda, A. Kajihara, T. Ohno, *Bull. Chem. Soc. Jpn.* **1984**, *57*, 405.

25 Y. Hisaeda, T. Nishioka, Y. Inoue, K. Asada, T. Hayashi, *Coord. Chem. Rev.* **2000**, *198*, 21.

26 H. Shimakoshi, A. Nakazato, T. Hayashi, Y. Tachi, Y. Naruta, Y. Hisaeda, *J. Electroanal. Chem.* **2001**, *507*, 170.

27 H. Shimakoshi, M. Tokunaga, Y. Hisaeda, *Dalton Trans.* **2004**, 878.

28 M. A. Jabbar, H. Shimakoshi, Y. Hisaeda, *Chem. Commun.* **2007**, 1653.

29 K. Tahara, H. Shimakoshi, A. Tanaka, Y. Hisaeda, *Tetrahedron Lett.* **2007**, *48*, 5065.

30 K. Tahara, H. Shimakoshi, A. Tanaka, Y. Hisaeda, *Dalton Trans.* **2010**, *39*, 3035.

31 Y. Murakami, Y. Hisaeda, *Bull. Chem. Soc. Jpn.* **1985**, *58*, 2652.

32 H. Shimakoshi, Y. Maeyama, T. Kaieda, T. Matsuo, E. Matsui, Y. Naruta, Y. Hisaeda, *Bull. Chem. Soc. Jpn.* **2005**, *78*, 859.

33 G. Fellenberg, *The Chemistry of Pollution*, Wiley, Chichester, **2000**, p. 123.

34 M. L. Hitchman, R. A. Spackman, N. C. Ross, C. Agra, *Chem. Soc. Rev.* **1995**, *24*, 423.

35 For a selected review of nanofiltration techniques, see: H. P. Dijkstra, G. P. M. van Klink, G. van Koten, *Acc. Chem. Res.* **2002**, *35*, 798.

36 A preliminary dialysis test revealed that a typical polypropylene membrane retained B_{12}–HBP **3** more effectively (ca. 80–85%) than the monomeric B_{12} **1** (ca. 35–40%) on the same scale as the electrolysis of DDT, indicating the promising property of the macromolecule **3** for ready removal from the product mixture.